The Accuracy of Remapping Irregularly Spaced Velocity Data onto a Regular Grid and the Computation of Vorticity

R.K. Cohn and M.M. Koochesfahani
Department of Mechanical Engineering, Michigan State University, East Lansing, MI

The velocity data obtained from Molecular Tagging Velocimetry (MTV) are typically located on an irregularly spaced measurement grid. In this method of velocimetry, the flowing medium is premixed with a molecular complex that can be turned into a long life-time tracer upon excitation by photons. The velocity vector is determined from the displacement of small regions "tagged" by a pulsed laser which are imaged at two successive times within the lifetime of the tracer. This technique may be viewed as the *molecular* counterpart of PIV. To take advantage of standard data processing techniques, the MTV data need to be remapped onto a regular grid with a uniform spacing. In this work we examine the accuracy and noise issues related to the use of various low order polynomial least-square fits for remapping and the subsequent computation of vorticity from these data. The information obtained has relevance to PIV data processing as well. As noted by Spedding and Rignot (1993), the best estimate of the location of the velocity vector acquired through the use of tracer techniques, such as PIV, is at the midpoint of the displacement vector. Thus, unless special care is taken, PIV data are also initially obtained on an irregular grid.

In the past, various methods have been used for remapping randomly spaced velocity data onto a regular grid. Among them are an inverse distance approach and a "global basis function" examined by Spedding and Rignot (1993). In this study, we consider the use of 2nd, 3rd, or 4th order polynomial to remap the velocity field by performing a local least-squares fit of the irregularly spaced data within region of radius R. This choice was selected based on the work of Agui and Jimenez (1987), who report that low order polynomial fits and "kriging" techniques produce the most accurate representation of the actual velocity field. However, no quantitative information on the performance of these methods is presented. Four approaches are assessed here for computing the out-of-plane vorticity field from the in-plane velocity measurements: direct differentiation of the polynomial fits used in the remapping process, 1st and 2nd order finite difference techniques (2nd and 4th order accurate, respectively) and an 8-point circulation method on the regular data. It should be noted that the 8-point circulation method is identical to the 1st order finite difference method after an appropriate choice of smoothing.

Several authors have examined the accuracy of the various means to compute vorticity from regularly spaced data. Spedding and Rignot (1993) used a 1st order finite difference technique for the inverse distance method or directly differentiating the global basis function. Results indicated that the global basis function produced generally superior results, however, results were found to be highly dependent upon the ratio, of a characteristic length scale, of the flow, L, to the mean spacing between measurements, δ. Abrahamson and Lonnes (1995) found that the circulation method resulted in slightly more accurate vorticity results than using a least-squares fit to a model velocity field. Luff *et al.*(1999) compared the 1st and 2nd order finite difference methods and an 8-point circulation method in the calculation of vorticity in the presence of both noise and missing data points. In terms of only the computed vorticity RMS, the 1st order finite difference technique produced the best results.

One short-coming of the above mentioned studies is that only the random component of the error field is examined. Fouras and Soria (1998) found that the error in the vorticity field could be

better represented if it is divided into two portions: a mean bias error due to spatial filtering, and a random error resulting from the propagation of error in the velocity measurements into the calculation of vorticity. In some cases, the mean bias error can be significantly larger than the random error. The Fouras and Soria study found that differentiating a 2nd order polynomial least-squares fit to the velocity data produced results superior to the 1st order finite difference approach. However, the results based on differentiating the fit were sensitive to the number of points used in the fit. This work was based entirely on regularly sampled velocity data; issues connected to remapping an irregular data set were not considered.

The aforementioned investigations suggest different optimum methods for vorticity computation depending on the criterion used to assess the error. In our work we directly compare several of the different vorticity calculation methods which were determined in the previous studies to produce the best results. In addition, we include the effect of remapping of the velocity field on the accuracy of vorticity estimation. The differentiation of the polynomial fit, used in remapping, as a means of estimating the vorticity is also considered. A simulation of an Oseen vortex, utilized by the previous studies, is also employed here as the basis for comparison. The effect of uncertainty in the velocity measurements in simulated by adding a random amount of noise to each velocity component.

Our simulations show that the accuracy of the remapping process depends on both L/δ and the normalized size of the region used in the least-squares fit, R/δ. The effect of increasing the value of R/δ on the velocity and vorticity fields is to decrease the random error, but increase the mean bias error. Generally, the decrease in random error is smaller than the increase in the bias error. All of the different polynomial orders tested produced accurate results in the remapping of the velocity field for suitable choice of L/δ and R/δ . For example, with $L/\delta > 4.5$ both the velocity mean bias error and random error are less than 1% of the peak velocity.

Results show that the most accurate vorticity results are achieved by either directly differentiating the 3rd order polynomial fit to the original irregular data or by the 2nd order finite difference technique. Note that this conclusion is different from previous studies because they either did not consider the 2nd order finite difference approach, or the performance was based only on the random error. For $L/\delta > 4.5$, we find the mean bias error and random error in vorticity can be less than 3% and 2%, respectively, of the peak vorticity. A decrease in L/δ causes a large increase in the vorticity bias error; error values higher than 18% of the peak vorticity are found for $L/\delta = 2.5$.

References:

Abrahamson, S. and Lonnes, S. [1995] "Uncertainty in calculating vorticity from 2D velocity fields using circulation and least squares approaches," *Exp. in Fluids*, **20**, pp. 10-20.

Agui, J and Jimenez, J. [1987] "On the performance of particle tracking," *J. Fluid Mechanics*, **186**, pp. 447-468.

Fouras, A. And Soria, J. [1998] "Accuracy of out-of-plane vorticity measurements from in-plane velocity field data," *Exp. in Fluids*, **25**(5/6), pp. 409-430.

Luff, J. D., Drouillard, T., Rompage, A. M., Linne, M. A. and Hertberg, J. R. [1999] "Experimental uncertainties associated with particle image velocimetry (PIV) based vorticity algorithms," *Exp. in Fluids*, **26**, pp. 36-54.

Spedding, G. R. and Rignot, E. J. M. [1993] "Performance analysis and application of grid interpolation techniques for fluid flows," *Exp. in Fluids*, **15**, pp. 417-430.

MIXED-MODE FRACTURE IN A RUBBERY PARTICULATE COMPOSITE

Timothy C. Miller
Air Force Research Laboratory, AFRL/PRSM, 10 E. Saturn Blvd. Edwards AFB, California, USA 93524

INTRODUCTION

Often cracks in rubbery particulate composites are found in the propellant grain of rocket motors and experience mixed-mode loading. These composites are made from a rubbery matrix with a high volume of rigid particles (70-80%). The cracks threaten structural integrity and can grow to catastrophic failure. Refinements in our predictive abilities yield cost savings by improving service life predictions. This work uses an approximate analysis to examine the crack behavior. This approach is practical and useful because it can be put to widespread use in industry.

EXPERIMENTAL PROCEDURE

We used center cracked specimens, 101.6 mm x 101.6 mm x 5.08 mm, with 25.4 mm center cracks oriented at an angle β with the horizontal. Different crack orientations provided specimens with different mode mixities. For these specimens, the phase angle of the complex stress intensity factor was approximately equal to the crack orientation angle β. We tested two specimens at each of the crack orientations (0°, 15°, 30°, 45°, and 60°), applying uniform vertical displacements to the horizontal specimen edges at a constant 5.08 mm/min rate. We measured the initiation loads and growth rates from videotape; we measured the initial growth directions from the fractured specimens after testing. The initiation loads were used with finite elements to determine the components (K_{IC} and K_{IIC}) of the initiation toughness.

RESULTS

We obtained all the results shown by applying linear elastic fracture mechanics concepts to a rubbery composite that has viscoelastic properties capable of high elongations. This approach is justified because the fracture initiation and growth occur on the linear part of the stress-strain curve and because moiré experiments show linear elastic behavior near cracks in these composite specimens. However, because of the time dependent constitutive behavior, the results must be applied to structures with similar nominal strain rates. This use of linear elastic fracture mechanics is practical because by greatly simplifying analyses that would otherwise be cumbersome and unfeasible it allows for widespread use.

The fracture toughness locus for the mixed-mode tests, shown in Figure 1, has an elliptical curve fit of the form:

$$\left(\frac{K_I}{K_{IC}}\right)^2 + \left(\frac{K_{II}}{K_{IIC}}\right)^2 = 1 \qquad (1)$$

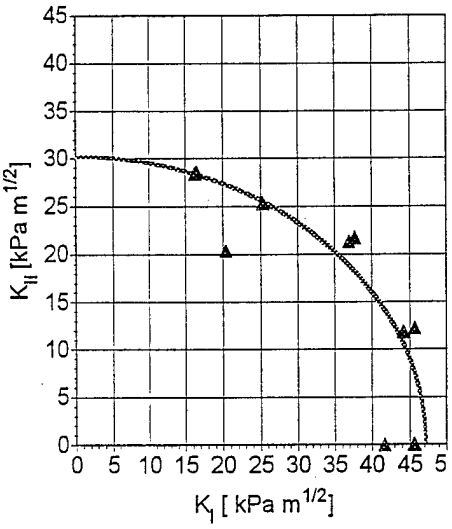

Figure 1 Elliptical failure locus

We treated the parameters K_{IC} and K_{IIC} as unknowns and determined them using least-squares. Equation (1) is regarded as linear in the unknowns $(1/K_{IC})^2$ and $(1/K_{IIC})^2$, and the least-squares method is applied using matrix algebra [1]. Researchers have used an elliptical curve fit previously for isotropic materials. Note that the pure mode II fracture toughness is smaller than its mode I counterpart. Previous explanations that examined the fracture toughness locus in relation to micromechanisms were based on observations from metals, and do not seem to apply to rubbery composites. Determining the connection to microstructure is left for future work, but two possibly relevant phenomena are suggested: the presence of rubbery ligaments behind the crack tip and the growth of voids from particles near the crack tip.

We used the experimentally determined loads with finite elements to determine the J integral and then to derive K_{IC} and K_{IIC}. Using the crack face displacement data, it was determined that for these specimens the complex stress intensity factor phase angles were approximately equal to the crack orientation angles. Then, using $J_c = K_c^2/E$, where K_c is

the magnitude of the complex fracture toughness, and $\Psi = \beta$, where Ψ is the phase angle, allows K_{IC} and K_{IIC} to be calculated.

The initial growth directions, or kink angles, were determined by experiment and are shown in Figure 2. This figure also shows predicted kink angles from several theories, all of which gave similar results [2,3]. The large deformations during actual loading made it difficult to unambiguously determine the kink angles, so we measured them after testing by projecting the fractured surfaces onto a large screen.

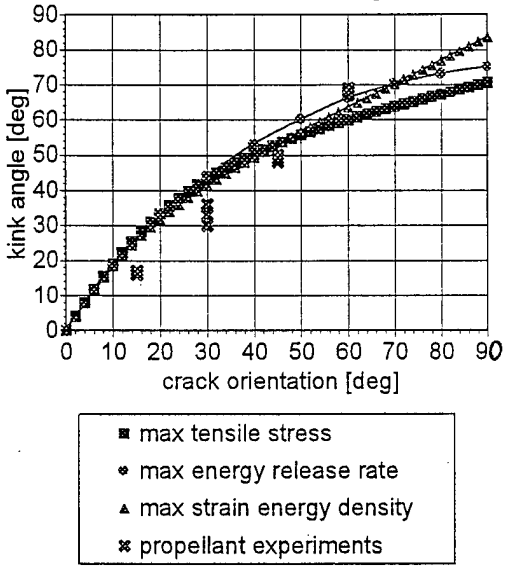

Figure 2 Kink angles vs. crack orientation angle

We measured the growth rates from videotape using the approach of Figure 3. During most of the growth, the angled crack of Figure 3a experiences mode I growth that can be characterized by the effective crack length and related mode I stress intensity factor of Figure 3b. The crack growth rate and K_I can be related through a power law relation such as:

$$\frac{da_{eff}}{dt} = CK_I^m \qquad (2)$$

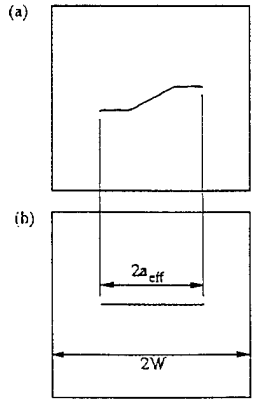

Figure 3 Modeling mixed mode crack growth

This gives nearly identical results for all the tested mode mixities. Because of this, the growth of a mixed-mode crack with a geometry shown in Figure 4a can be modeled using the simplified geometry of Figure 4b. Figure 5 shows the aggregate data and resulting curve fit; the parameters in eqn (2) are $C = 1.79 \times 10^{-6}$ and $m = 2.73$. Results for a mode I specimen gave the nearly identical results of $C = 1.85 \times 10^{-6}$ and $m = 2.74$.

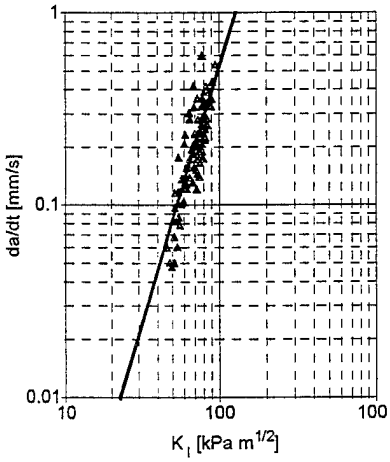

Figure 5 Effective crack growth rate vs. K_I

CONCLUSIONS

Although rubbery particulate composites have viscoelastic properties, high elongations, and complicated failure mechanisms, they can be studied, for a given nominal strain rate, using the principles of linear elastic fracture mechanics. When analyzed like this, the fracture locus is elliptical. The initial crack growth angles match the strain energy density predictions best, although for all but the highest mode mixities, other theories gave nearly identical results. The crack growth rates can be predicted using an approximate mode I approach. The result is a simple approach that circumvents more detailed and difficult analyses. Future work could include experimental methods to study the causes of fracture in these composites, especially the micromechanisms near the crack tip at various mode mixities.

REFERENCES

1 Sanford, R. J. Application of the Least-Squares Method to Photoelastic Specimens. *Exp. Mech.*, 1980, **20**, 192-197.

2 Erdogan, F. and Sih, G. C. On the Crack Extension in Plates under Plane Loading and Transverse Shear. *J. Basic Engineering*, 1963, **85D**, 519-527.

3 Sih, G. C. and Chen, E. P. *Cracks in Composite Materials*. Martinus Nijhoff, The Hague, 1981.